*Proceedings of the Korean Nuclear Society Spring Meeting*
*Kwangju, Korea, May 1997*

# PREDICTION OF THE ONSET OF SLUG FLOW IN NEARLY HORIZONTAL AIR-WATER COUNTERCURRENT FLOW

**Seon-Oh Yu and Moon-Hyun Chun**
Korea Advanced Institute of Science and Technology

**Yang-Seok Kim**
Korea Electric Power Research Institute

## ABSTRACT

*The transition from a statified wavy to a slug flow has been analyzed considering the mechanistic forces acting on the wave crest in a nearly horizontal air-water countercurrent flow. To verify the results of the analysis, a series of experiments have been performed changing the inclination angle of the test section. Comparisons of the theoretical predictions with experimental data show a good agreement and the results show that the present model gives similar results of Taitel and Dukler's in the case of inclined pipes. However, at high superficial liquid velocity, the results of present work agree more closely with data than that of Taitel and Dukler's. Also, predictions of the present model gives a very close agreement with the experimental data for various tube sizes obtained by others.*

## 1. INTRODUCTION

The countercurrent two-phase flow occurs in many industrial processes and nuclear power systems under a LOCA condition in particular. The stability of this countercurrent flow is very important because there is a potential to limit the delivery of ECC water to the hot reactor core during a LOCA. Particulary if a water slug is generated in the pipe, this may initiate a water hammer when the main feed water pump is stopped. Therefore, it is very important to have a complete knowledge on the thermal-hydraulic interactions of this countercurrent flow for the quantitative analysis of the course of the accident and the stability analysis of the flow. Over the past years, the modeling and the thermal-hydraulic analysis of two-phase flow have been carried out in connection with the safety analysis of nuclear reactor systems. It is well established now that the two-phase flow takes on many different forms, which are known as flow patterns or flow regimes.

Although the subject of transition condition to slug flow has been extensively studied over the last fifty years, its complete analysis has not been obtained yet. The main objective of the present work is to determine the transition condition to a slug flow in nearly horizontal countercurrent stratified wavy flow considering the interfacial shear work acting on the wave crest. There are several competing forces acting on the wave and the major forces that may bring the instability of the flow are analyzed here. In addition, a series of experiments have been performed to investigate the transition from a stratified to a slug flow in a nearly horizontal test section of 0.05 m diameter and 2 m in length under atmospheric pressure condition.

## 2. ANALYSIS OF TRANSITION CONDITION FOR TWO-PHASE FLOW

Figure 1 shows a schematic diagram of ideal waves with sudden void fraction change from $\bar{\alpha}$ to $\alpha'$, when the test section has an inclination angle of $\theta$. It is assumed that the wave has a cosine form. Generally, the transition from a stratified wavy flow to a slug flow occurs when the lifting forces acting on a wave crest exceed the opposing forces acting on the interfacial surface, i.e., $\sum F_{lofting} > \sum F_{lowering}$. As pointed out by Wallis and Dobson [1], gas phase depressurization due to acceleration may be the cause of the lifting force when gas crosses over the wave crest. From the Bernoulli equation, the pressure change across the wave crest is obtained as follows:

$$\Delta P_d = \frac{1}{2}\rho_g V_g^2\left[\left(\bar{\alpha}/\alpha'\right)^2 - 1\right] + g\,\rho_g\left[h(\alpha') - h(\bar{\alpha})\right]\sin\theta . \tag{1}$$

Minato et al. [2] suggested that the change of the liquid kinematic energy over the wave crest contributes to the lifting force and proposed a force to promote wave growth as follows:

$$\Delta P_k = \frac{1}{2}\rho_l V_l^2 \frac{(2-\bar{\alpha}-\alpha')(1-\bar{\alpha})}{(1-\alpha')} . \tag{2}$$

Another lifting force adopted here is the interfacial shear stress in the $y$-direction on the wave crest:

$$W_\tau = \int_t S_i\, \Delta l\, \tau_{i,y}\, V_r\, dt = \frac{\pi}{4\kappa}\rho_g f_i\, S_i\, \eta_0\, V_r^2 \tag{3}$$

where $\tau_{i,y}$ is the interfacial shear stress in the y-direction, $\Delta l$ is the length of wave crest where the interfacial shear stress acts, and $V_r$ is the relative velocity. Then, $\Delta P_\tau$, the force that promotes the wave growth and which originates from the interfacial shear stress, can be obtained as follows:

$$\Delta P_\tau = \frac{\pi}{4\kappa}\rho_g f_i\, S_i\, \eta_0\, V_r^2 \frac{1-\alpha'}{\bar{\alpha}-\alpha'} . \tag{4}$$

Next, the forces that act to lower the interfacial surface waves are the gravity and the surface tension, but the latter of the two forces is negligibly small in the case of large waves. The gravity force can be expressed as

$$\Delta P_g = g(\rho_l - \rho_g)\left[h(\alpha') - h(\bar{\alpha})\right]\cos\theta . \tag{5}$$

The net lifting force that promotes the wave growth can be expressed as a function of $\alpha'$ and $\bar{\alpha}$:

$$L(\alpha',\bar{\alpha}) = \Delta P_d + \Delta P_k + \Delta P_\tau - \Delta P_g . \tag{6}$$

Figure 2 shows the numerical procedure to obtain the transition boundaries from a stratified to a slug flow using Eq. (6).

## 3. EXPERIMENTAL WORKS

A series of countercurrent stratified air–water flow experiments have been performed to obtain experimental data to compare with the present theoretical analysis performed to predict the transition conditions from a stratified to a slug flow. Figure 3 shows a schematic diagram of the test facility which consists of a test section, an air–water supply systems, instrumentations, and data acquisition system. The test section is made of an acrylic tube (2 m in length and 0.05 m in inner diameter) for flow visualization whose both ends have a simple sharp-edge. Three different inclination angles (i.e., $\theta$ = 0.4°, 1°, 2° from the horizontal) have been employed to examine the effect of inclination angle on the flow transition condition. The flow rates of air and water are monitored by rotameters. The water levels have been measured using parallel-wire conductance probes that have about 0.50 mm of standard deviation, and the pressure drop of the gas phase has been measured by the differential pressure transmitter (with a full scale of 0.05 m water column) which has an accuracy of ±0.025 %.

A series of experiments have been carried out with fixed water flow rate while increasing the air flow rate by small increments until the large wave crest reaches the upper inner surface of the test section. For all the tests, sufficient time is allowed to achieve a quasi-steady state, and the change of wave forms following the increase in gas phase velocity are observed. A similar procedure is repeated for various water flow rates and with different inclination angles of test section. In the present works, the ranges of the superficial water velocity, $j_l$, and the superficial air velocity, $j_g$, are 0.01273 ~ 0.13581 *m/s* and 0.679 ~ 6.791 *m/s*, respectively. All the tests are conducted at atmospheric condition, and during each test, the air and water temperatures are kept in the range of 23 ~ 24 °C and 20 ~ 22 °C, respectively.

## 4. RESULTS AND DISCUSSION

To calculate the interfacial shear stress, following interfacial friction factor proposed by Lee [3] is used

$$f_i = 4.13\times10^{-11}\,\mathrm{Re}_g^{0.96}\,\mathrm{Re}_l^{0.31}\left(\mu_l/\mu_g\right)^{1.86}. \qquad (7)$$

This correlation includes the viscosity ratio. According to the experimental results, the interfacial friction factor depends strongly on the viscosity ratio as well as the gas Reynolds number, and it is a weak function of the liquid Reynolds number. In Fig. 4, the present experimental data are compared with the Lee's correlation. It can be observed that the Lee's correlation agrees with the present data within −30 ~ +20 %.

Figure 5 shows the typical results of $L(\alpha',\bar{\alpha})$. The wave grows while the net lifting force is positive. When specific velocities are small enough, the stratified smooth, wavy, and roll wavy patterns are predicted as shown by the curves of (a), (b), and (c) in Fig. 5. When the gas phase velocity is increased gradually, the flow pattern changes from a stratified wavy to a slug flow as shown by the curve (d), which shows that the wave begins to grow towards the top of the tube wall. These flow pattern transitions obtained from the present work agree with visual observations shown in Fig. 6.

Figure 7 (a) shows theoretical predictions and experimental results for transition boundaries from a stratified to a slug flow in the test section. The difference between the predicted and the experimental results is within max. 25 %. In Fig. 7 (b), predicted values are compared with the experimental results reported by No and Choi [4]: Predictions of the present model for different tube sizes and for various inclination angles are fairly close to the data. Also Taitel and Dukler [5] model predictions are compared with data in Fig. 7. The results of present model have similar trends with those of Taitel and Dukler's. However, at high superficial liquid velocity, the present model gives a better agreement with experimental data.

In addition, to investigate the effects of work done by the shear stress, another interfacial friction factor correlation of Lee and Bankoff [6] is used. The results obtained by using Lee and Bankoff's correlation give similar results as obtained by Lee's correlation which is shown in Fig. 8. However, it is found that the results of Lee and Bankoff's correlation overpredict the transition condition for the low superficial liquid velocity. The reason for this can be explained as follow: The intensity of wave height fluctuation is very sensitive to the gas Reynolds number as well as the liquid Reynolds number for both air–water and steam–water flow. The intensity of steam–water flow is several times larger than that of air–water flow, which is due to the effect of the liquid viscosity [3]. Therefore, it is not surprising that the results obtained by Lee's correlation that includes the viscosity ratio give better agreement with data than those obtained by Lee and Bankoff's based on the steam–water data.

## 5. CONCLUSIONS

A mechanistic model for transition from a stratified wavy to a slug flow in a pipe has been developed for air–water countercurrent flow. The present mechanistic model has incorporated the effect of the interfacial shear stress acting on the wave including other factors considered by previous authors, i.e., the effects of gas phase depressurization, liquid kinematic energy, and gravity force.

It is found that the present model can satisfactorily predict the transition boundaries from a stratified wavy to a slug flow for the case of different inclined angles and different diameters of the test section. Present model gives a better results than those of Taitel and Dukler's at high liquid superficial velocity in particular.

## REFERENCES


1. Wallis, G. B. & Dobson, J. E., "The onset of slugging in horizontal stratified air-water flow," *Int. J. Multiphase Flow* **1**, 173-193 1973.
2. Minato, A., Ikeda, T., & Naitoh, M., "Mechanistic Model of slugging onset in horizontal circular tube," *J. Nuclear Science and Technology* **23,** 761-768, 1986.
3. Lee, S. C., "Interfacial friction factor in countercurrent stratified two-phase flow," *Chem. Eng. Comm.* **118,** 3-16, 1992.
4. No, H. C. & Choi, K. Y., "Experimental studies of flooding in nearly horizontal pipes," *Int. J. Multiphase Flow* **21.** 419-436, 1995.
5. Taitel, Y. & Dukler, A. E., "A model for predicting flow regime transition in horizontal and near horizontal gas-liquid flow," *AIChE J.* **22,** 47-55, 1976.
6. Lee, S. C. & Bankoff, S. G., "Stability of steam–water countercurrent flow in an inclined channel: flooding," *J. Heat Transfer* **105**, 713-718, 1983.

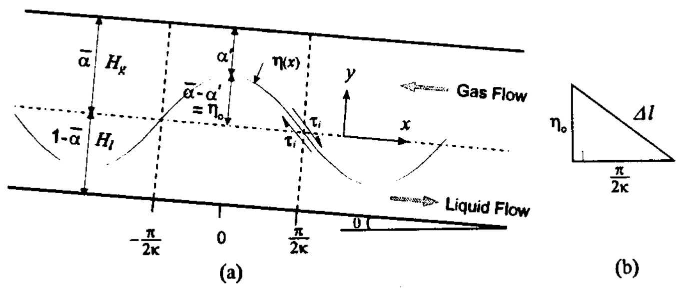


Figure 1. Flow configuration and notation.

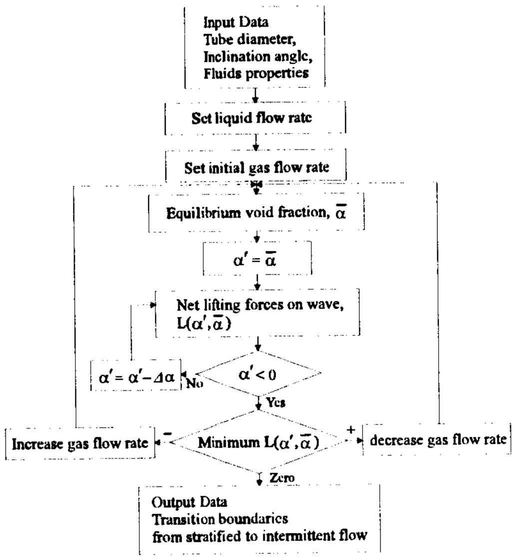


Figure 2. Numerical calculation procedure for net lifting force.

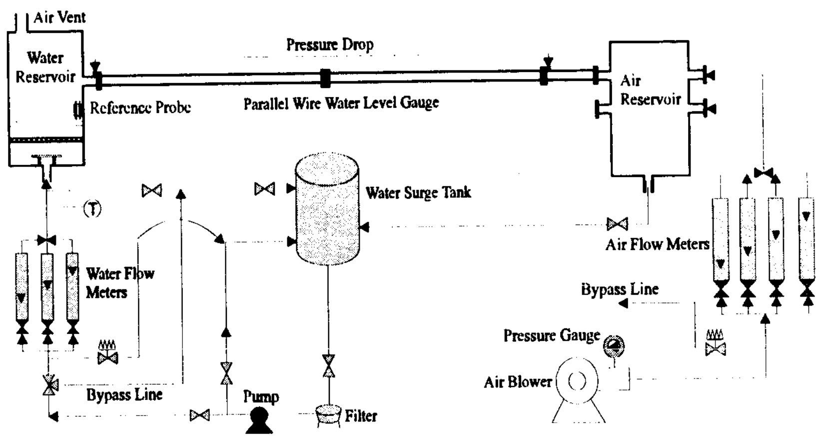


Figure 3. Schematic diagram of experimental apparatus.

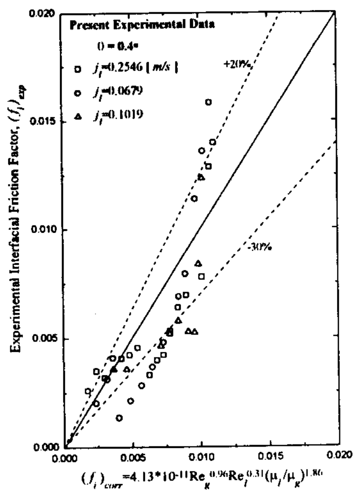


Figure 4. Comparison of interfacial friction factor between present experimental data and Lee's correlation.

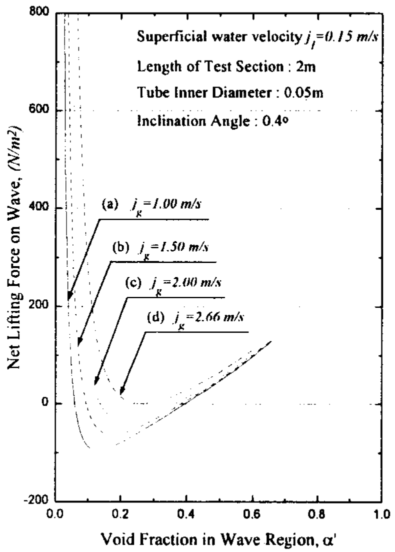


Figure 5. Relationship between lifting force on wave and void fraction in air-water countercurrent flow.

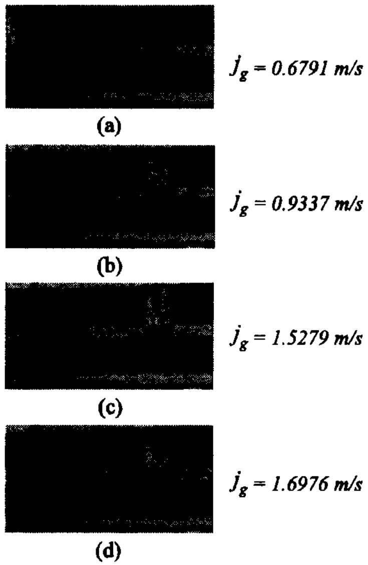


Figure 6. Photographs showing the change of wave pattern ($j_l$ = 0.1358 m/s).

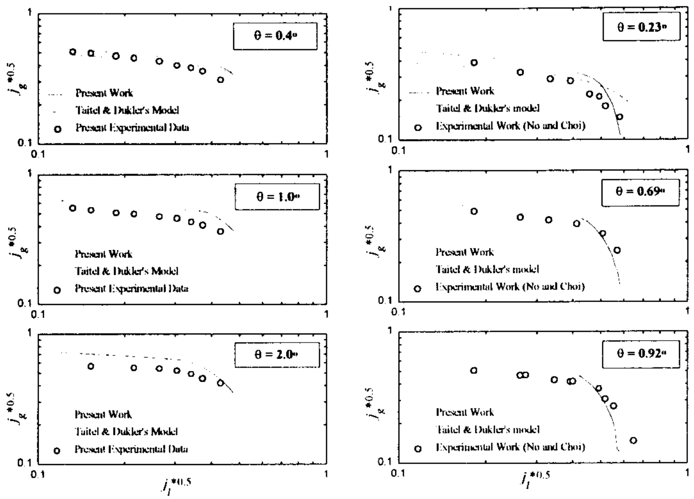


(a) (b)

Figure 7. Comparison between predicted and experimental data.

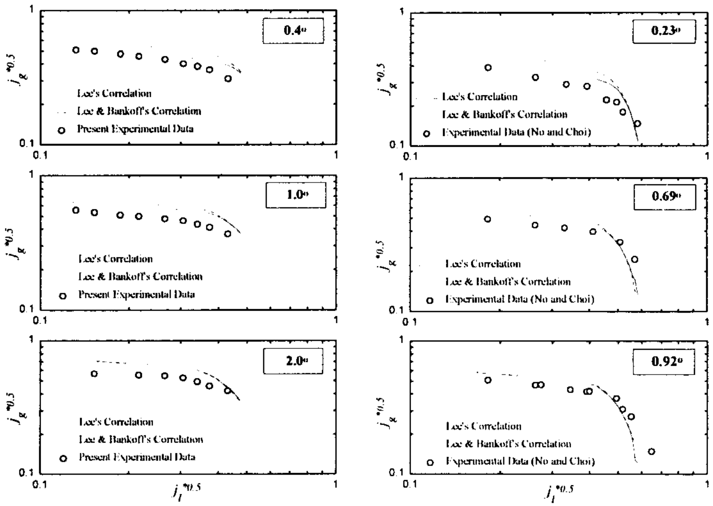


(a) (b)

Figure 8. The effect of the interfacial friction factor.